Chapter 6
Influence of Geometry and Loading Direction on the High Strain Rate Compression Response of modified GLARE Laminates

Muddu Rahul Bharadwaj*, **Rohit Kumar, Palak Bhagoria, and Vikrant Tiwari**

Abstract Fiber Metal Laminates (FMLs) are utilized across various applications because of their important benefits, which include high impact resistance, low density, and high strength to weight ratio. In this work, the compression behavior of plain-woven S-glass fiber-reinforced laminate interspersed with AA8011-H14 aluminum sheets (modified GLARE) under high strain rate loading is investigated using Split Hopkinson Pressure Bar (SHPB). The FML was produced using the vacuum-assisted resin transfer method. Under out-of-plane compression, two distinct specimen geometries—cuboidal and cylindrical— were examined at various strain rates ranging from 300 to 2000 s^{-1}. Additionally, rectangular specimens were also used to assess FML's dynamic compressive response in the in-plane direction. The results showed an increase in the compressive strength with strain rate for both the specimen geometries, yet in comparison, the cylindrical specimens exhibited a slightly higher strength to their rectangular counterparts at high strain rates due to better stress distribution. Delamination and fiber matrix cracking were the main failure modes for both the geometries. However, even at low strain rates, in cuboidal specimens localized failures, such as edge shear and corner cracking were observed. For the in-plane loading of rectangular specimens, metal layer buckling and plastic deformation dominated at lower strain rates, whereas brittle fracture of fibers and cracking in aluminum layers were seen at higher strain rates for the in-plane configuration.

Keywords FiberMetalLaminate · GLARE · SHPB · High strain rate

Introduction

Fiber Metal Laminates (FMLs) are a promising class of hybrid composite materials that offer the unique combination of properties of both metals and composites. The earliest evidence of FMLs can be dated back to the 1980s at the Delft university with the development of Aramid fiber reinforced Laminate (ARALL) which is an aluminium laminate reinforced with aramid fibers [1, 2]. Further development in this field with various FMLs made from other materials [3, 4] led to the production of Glass Fiber Reinforced Aluminum Laminates (GLARE). GLARE panels find numerous applications in aerospace, defense and marine industries due to their specific weight to strength ratio and their better adhesion properties compared to ARALL [5]. Due to these favorable properties, various researchers have studied the characterization of GLARE laminates subjected to uni-axial loading conditions [6, 7]. Most of the studies took help of the properties of individual constituents like Glass Fiber Reinforced Plastic (GFRP) [8], thermosetting or thermoplastic polymer used for adhesion [9] and the metal layers. Techniques like Digital Image Correlation (DIC) have also been employed in experiments along with numerical analysis [10, 11]. The dynamic characterization of these is also very crucial due to their nature of application. However, most experiments in the dynamic strain rate range focused on the tensile and impact resistance of the GLARE laminates [12–14]. For instance, Sharma et al. [12] studied the behavior of GLARE laminates with modifications to their thickness under high strain rate tensile loading. The FMLs showed strain rate sensitive behavior at high strain rates and the strength was shown to increase by 60% compared to the quasi-static loading conditions. Zhou et al. [13] along with high strain rate tensile experiments, have extended their study to low velocity impact tests on specimens made from modified GLARE by using different metal alloys. Their findings showed a contrast of low-strain rate sensitivity for the range of strain rates considered.

Muddu Rahul Bharadwaj · Rohit Kumar · Palak Bhagoria · Vikrant Tiwari
Department of Applied Mechanics, Indian Institute of Technology Delhi, New Delhi, India, 110016
e-mail: rahulbharadwaj95@gmail.com; rohitnituk001@gmail.com; palakbhagoria@gmail.com; Vikrant.Tiwari@am.iitd.ac.in

Paul Allison et al. (eds.), *Dynamic Behavior of Materials, Vol. 1*, Conference Proceedings of the Society for Experimental Mechanics Series, https://doi.org/10.13052/97887-438-0827-5_6

In this study, efforts have been made to study the dynamic behavior of modified GLARE laminate which is made from plain-woven S-glass fiber reinforcement and AA8011-H14 aluminium sheets. The geometrical effect of the typical cylindrical vs cuboidal specimens was investigated at high strain rates of 300 – 2000 s^{-1}. Additionally, these cuboidal specimens were also subjected to in-plane loading conditions along the thickness direction and the failure types were observed and reported.

Methodology

Split Hopkinson Pressure Bar (SHPB) or Kolsky bar is a commonly used technique to evaluate the material's response at high strain rates. The SHPB used in this study consists of three bars, namely, the incident, transmission and striker bar, all made of titanium (Ti-6Al-4V) material. Working principle of the SHPB is very well documented by many researchers [15, 16]. The strain vs time signals obtained from the data acquisition system of the SHPB setup are further used to calculate the average stress (σ_s) – strain (ε_s) relation and the strain rate ($\dot{\varepsilon}$) of the specimen using the following equations [17].

$$\dot{\varepsilon} = \frac{2C_b}{L_s}\varepsilon_r \tag{1}$$

$$\sigma_s(t) = \frac{A_b E_b}{A_s}\varepsilon_t(t) \tag{2}$$

$$\varepsilon_s = \frac{2C_b}{L_s}\int_0^t [\varepsilon_r(t)]\, dt \tag{3}$$

Here, C_b, E_b, A_b, represent the wave velocity, Elastic modulus and area of the bar respectively. A_s, L_s are the area and length of the specimen respectively. ε_r,ε_t are the reflected and transmitted strain signals and *t* being the time. A typical strain signal obtained from the SHPB experiments is shown below (Fig. 1) along with the force equilibrium that is achieved over both ends of the specimen.

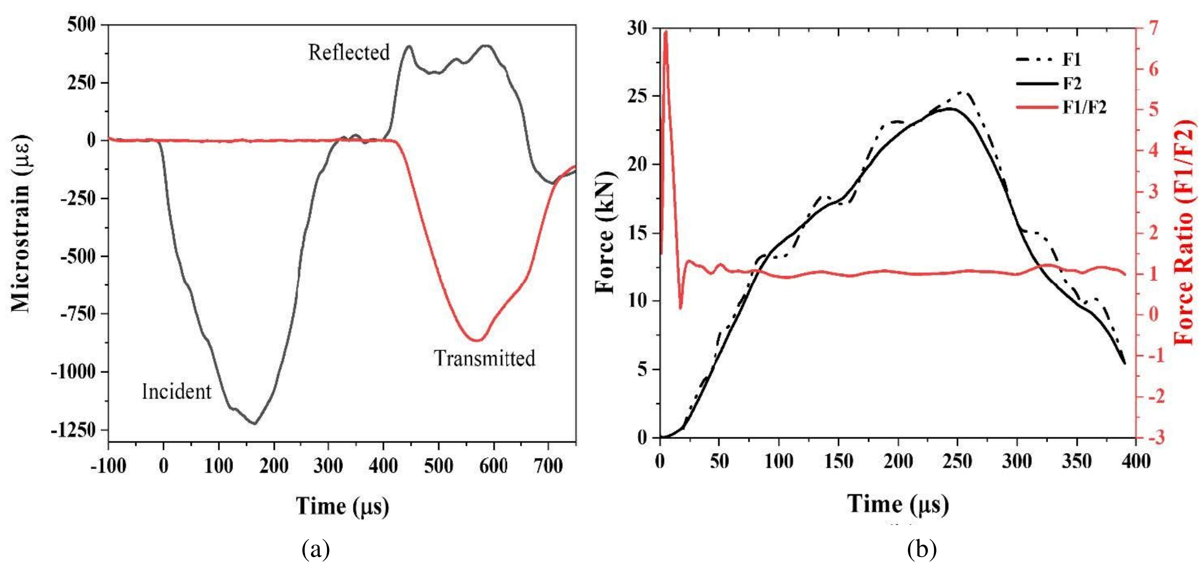

Fig. 1 (**a**) Strain – time history and (**b**) force equilibrium of a typical experiment

The FML utilized for this study was prepared using Vacuum Assisted Resin Transfer Molding (VARTM) method. It consists of 4 layers of AA8011-H14 sheets of thickness 0.5 mm each and 3 composite layers (Fig. 2). Each composite layer is made up of five plain woven S-glass fabric sheets bonded with two-part epoxy resin system (EPOFINE® −1564/FINEHARD-3486–2) supplied by Fine Finish Organics Pvt. Ltd, Mumbai. The metal volume fraction was 0.6, while the remaining 0.4 fraction, which included fiber and epoxy, had the fiber volume fraction of 0.6. The final dimensions of the FML so produced were 300 mm by 300 mm by 6 mm. The samples required for dynamic compression were prepared using high pressure waterjet cutting. The dimensions of cylindrical and cuboidal specimens so produced were 12 mm (diameter,

Fig. 2 Cuboidal and cylindrical specimens used in the study showing the layup sequence

D) by 6 mm (thickness, L) and 11 mm by 11 mm by 6 mm respectively. The L/D ratio for out-of-plane experiments was maintained to be 0.5.

Results and Discussion

Out-of-Plane Loading

The out-of-plane compression experiments were done on SHPB for both cylindrical and cuboidal specimens at various strain rates ranging from 300 – 2000 s^{-1}. For ease of comparison and data analysis, the strain rates were divided into low, medium and high strain rate regimes within the range: 300 – 900 s^{-1}, 900 – 1500 s^{-1}, 1500 – 2000 s^{-1} respectively. The stress – strain response of cylindrical and cuboidal specimens for three different strain rates is shown in Fig. 3.

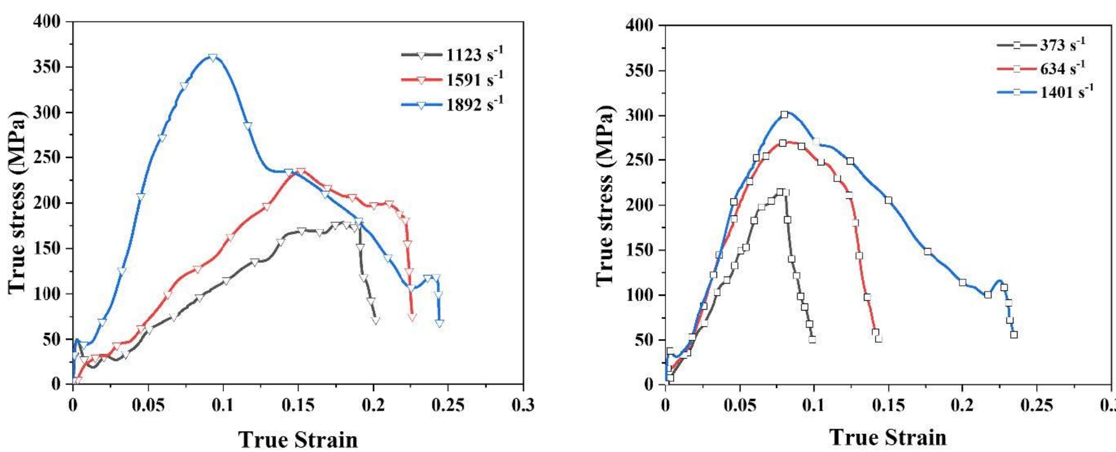

(a) (b)

Fig. 3 Stress – strain response of (**a**) cylindrical and (**b**) cuboidal geometry specimens at various strain rates

Both geometries showed positive strain rate sensitivity. For cylindrical specimens, in the initial linear elastic region, the slope remained almost constant indicating stiffness is relatively insensitive to strain rate. Also, the final failure is different at higher strain rate regime with a more pronounced dip indicating brittle failure compared to the more progressive failure at low and mid strain rate regimes. For the cuboidal specimens, a similar trend of stiffness insensitivity to strain rate was observed. However, the initial slope was a little steeper compared to their counterparts. The post yield hardening response also was more rapid and pronounced possibly due to non-axisymmetric shape. Nevertheless, the primary reason for failure was found to be delamination and fiber matrix cracking for both the geometries. A power law model, as shown in Eq.4, was used to find out the relation between ultimate strength (σ_{ult}) and strain rate ($\dot{\varepsilon}$) for both the geometries.

$$\sigma_{ult} = C\dot{\varepsilon}^{\beta}. \quad (4)$$

C is the proportionality constant and β is the strain rate sensitivity parameter. The ln σ_{ult}- ln $\dot{\varepsilon}$ plots for both the geometries can be seen in Fig. 4. As exhibited earlier, both geometries have positive strain rate sensitivities. However, the cylindrical specimens have shown higher strain rate sensitivity than the cuboidal ones. All these parameters for the linear curve fit are shown in Table 1.

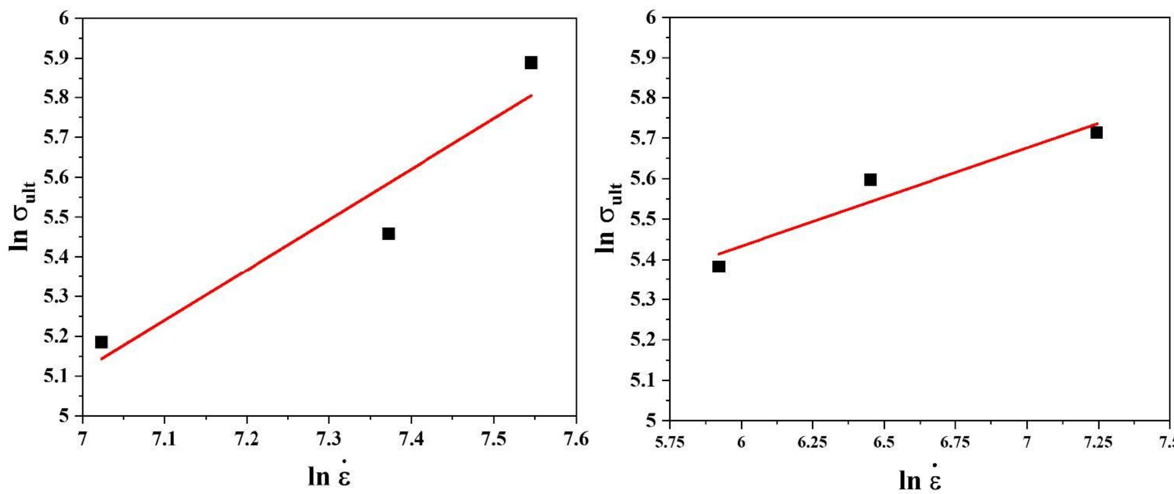

(a) (b)

Fig. 4 ln-ln plots of stress vs strain rate for (**a**) cylindrical and (**b**) cuboidal specimens along with a linear fit

Table 1 Parameters of curve fitting used in Fig. 4 for cylindrical and cuboidal specimens

Equation: y = a + b*x		
	Cylindrical	***Cuboidal***
Intercept (a)	-3.76214 ± 3.06711	3.97603 ± 0.46552
Slope (b)	**1.26787 ± 0.41918**	**0.24282 ± 0.07094**
R-Square (COD)	**0.90146**	**0.92136**
Residual Sum of Squares	0.0248	0.00446

Using the above linear fit parameters, the ultimate stresses for the missing strain rates in various regimes were extrapolated and found out. A new dimensionless parameter called strength ratio (σ_o^*), defined as per the following equation to facilitate comparison, is used.

$$\sigma_o^* = \frac{\sigma_{cylindrical}}{\sigma_{cuboidal}}. \tag{5}$$

It has been found that the cuboidal specimens generally reached the higher peak stress values at lower strain rates, indicating their earlier failures and stress concentrations at edges and corner cracking. This parameter has been plotted against the strain rate for a better understanding of its sensitivity (Fig. 5). As the strain rate increased, the value of strength ratio which was less than one slowly rose to higher than 1 which shows the sustained strain hardening effects in cylindrical specimens. A polynomial fit was determined to best describe its variation indicating a non-linear sensitivity to strain rate. The parameters of the curve fit are given in Table 2.

Table 2 Polynomial curve fit parameters of strength ratio from Fig. 5

Equation	y = C1 + B1*x^1 + B2*x^2
Intercept (C1)	**0.09808 ± 0.14398**
B1	**2.75051E-4 ± 2.97016E-4**
B2	**1.17312E-7 ± 1.31222E-7**
R-Square (COD)	**0.969**
Residual Sum of Squares	**0.01554**

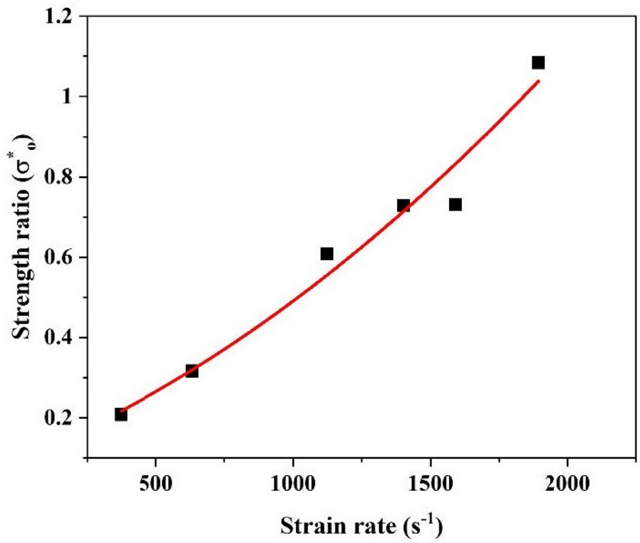

Fig. 5 Strength ratio vs strain rate with a polynomial fit.

In-Plane loading

The cuboidal specimens were also loaded along the warp direction (in-plane loading) i.e. along the thickness direction to study the effect of dynamic compression at various strain rates ranging from 600 – 1500 s^{-1}. Although the effective area is reduced, the volume of the material remains constant. Hence, an effort has been made to study their behavior and compare them with out-of-plane cuboidal specimens. The stress – strain plots of the cuboidal specimens loaded along the in-plane direction are shown in Fig. 6 (a). A similar attempt to find out the strain rate sensitivity of in-plane loaded is made using the Eq. 4 and the ln σ_{ult}- ln $\dot{\varepsilon}$ is plotted (Fig. 6 (b)). Through a linear fit, the strain rate sensitivity parameter (β) is found out and compared to that of the out-of-plane loaded specimens (Table 3). Buckling/bending of aluminum layers at lower strain rates was observed as the primary failure mechanism during this loading. The strain-to-failure and the peak stress achieved through this loading are comparatively lower, indicating early failures of aluminum due to its thickness. Furthermore, higher localization of deformation and cracking was observed within the metal parts of the FML, suggesting their instability, along with fiber cracking as the strain rate increased.

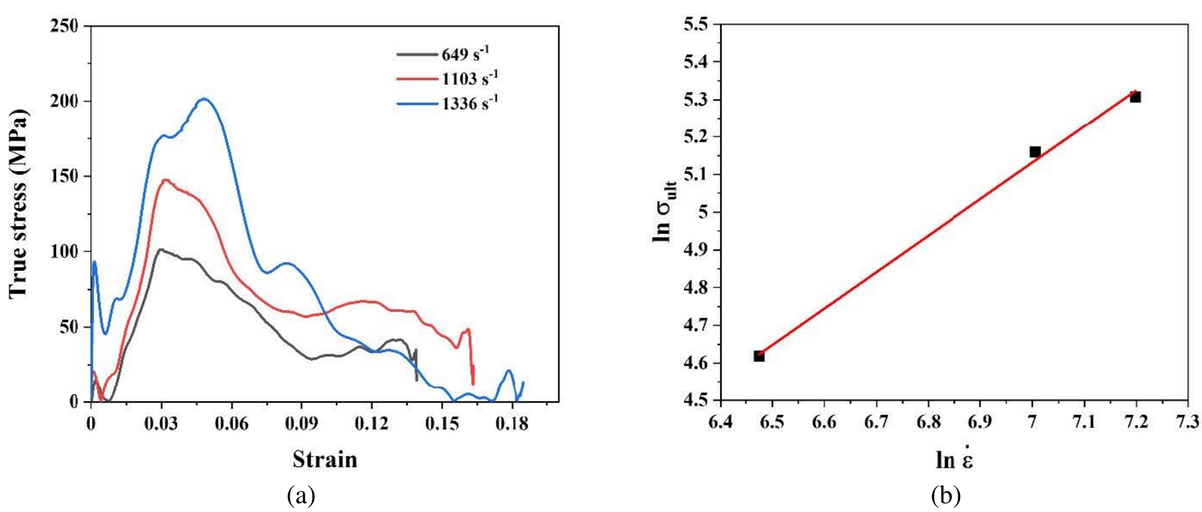

Fig. 6 (**a**)Stress - strain response and (**b**) stress - strain rate behavior of Cuboidal samples in in-plane loading

The strain rate sensitivity is higher than the out-of-plane loading conditions as can also be observed from the stress-strain plots which show a very steep increase in the peak stress values.

Table 3 Linear curve fit parameter from Fig. 5

Equation	y = a + b*x
Intercept	**-1.64263 ± 0.36314**
Slope	**0.96771 ± 0.05263**
R-Square (COD)	**0.99705**
Residual Sum of Squares	7.74975E-4

CONCLUSION

This study was aimed at finding out the effect of geometry and loading direction of high strain rate compression response of AA8011/ Plain woven S-Glass fiber epoxy modified GLARE laminates. The experiments were carried out in the range of 300 – 2000 s^{-1} initially for both cylindrical and cuboidal specimens along ot-of-plane loading direction. The strain sensitivity parameter was found out using power law model with the best fit being linear. At lower strain rates, although cuboidal specimens had higher peak stress values, with increase in strain rate this trend was reversed, indicating their very low strain rate sensitivity. The damage too was more progressive in case of cylindrical specimens with stress uniformity compared to the more brittle nature and steep rise in plastic zones observed in cuboidal specimens due to their non-axisymmetry. The major damage mechanism was the delamination of the metal and composite layers in both the geometries. Further, in-plane loading experiments were also conducted on the cuboidal samples along the warp (thickness direction) for strain rates of 600 – 1500 s^{-1}. The strain rate sensitivity was on par with the out-of-plane cylindrical experiments except the strain to failure and peak stress values being very low. Buckling of the aluminum layer and fiber fracture were the dominating failure mechanisms in this direction of loading.

References

1. Vermeeren CA, "An historic overview of the development of fibre metal laminates", *Applied Composite Materials*,10:189-205, 2003.
2. Vlot A, Gunnink JW, "Fibre metal laminates: an introduction", *Springer science & Business Media*, 2011.
3. Asundi A, Choi AY,"Fiber metal laminates: an advanced material for future aircraft", *Journal of Materials processing technology*, 63(1-3):384-94, 1997.
4. Cantwell WJ, "The mechanical properties of fibre-metal laminates based on glass fibre reinforced polypropylene", *Composites science and technology*, 60(7):1085-94, 2000.
5. Young JB, Landry JG, Cavoulacos VN, "Crack growth and residual strength characteristics of two grades of glass-reinforced aluminium 'Glare"', *Composite Structures*, 27(4):457-69, 1994.
6. Sharma AP, Khan SH, Parameswaran V, "Experimental and numerical investigation on the uni-axial tensile response and failure of fiber metal laminates". *Composites Part B: Engineering*. 125:259-74, 2017.
7. Ergun H, Liaw BM, Delale F, "Experimental-theoretical predictions of stress–strain curves of glare fiber metal laminates", *Journal of Composite Materials*, 52(1):109-21, 2018.
8. Song B, Chen W, Weerasooriya T, "Quasi-static and dynamic compressive behaviors of a S-2 glass/SC15 composite", *Journal of Composite Materials*,37(19):1723-43, 2003.
9. Kumar R, Bhagoria P, Bharadwaj MR, Tiwari V, "From quasi-static to dynamic: Experimental study of mechanical and fracture behaviour of epoxy resin", *International Journal of Impact Engineering*.195:105101, 2025.
10. Academic Block, "Image Based Measurement and Analysis", *https://www.academicblock.com*, 2023.
11. He W, Wang C, Wang S, Yao L, Wang L, Xie D, "Characterizing and predicting the tensile mechanical behavior and failure mechanisms of notched FMLs—Combined with DIC and numerical techniques", *Composite Structures*, 254:112893, 2020.
12. Sharma AP, Khan SH, Parameswaran V, "Response and failure of fiber metal laminates subjected to high strain rate tensile loading", J*ournal of Composite Materials*, 53(11):1489-506, 2019.
13. Zhou J, Guan ZW, Cantwell WJ, "The influence of strain-rate on the perforation resistance of fiber metal laminates", *Composite structures*,125:247-55, 2015.
14. Khan SH, Sharma AP, Kitey R, Parameswaran V, "Effect of metal layer placement on the damage and energy absorption mechanisms in aluminium/glass fibre laminates", *International Journal of Impact Engineering*, 119:14-25, 2018.
15. Chakraborty P, Pandouria AK, Singha MK, Tiwari V, "Constitutive behavior of AA7475-T7351 at high strain rate and elevated temperatures", *Dynamic Behavior of Materials*, Volume 1: Proceedings of the 2020 Annual Conference on Experimental and Applied Mechanics 2021 (pp. 15-23), Springer International Publishing.
16. Pandouria AK, Yadav K, Tiwari V, "Compressive and tensile behavior of AA2014-T6 under different strain rates and different temperatures", *Structures*, Vol. 49, pp. 12-25, Elsevier. 2023.
17. Chen WW, Song B, "Split Hopkinson (Kolsky) bar: design, testing and applications,"*Springer Science & Business Media*, 2010.